Oil & Gas Science and Technology – *Rev. IFP,* Vol. 63 (2008), No. 4, pp. 553-561

DOI: 10.2516/ogst:2008036

Dossier

Diesel Engines and Fuels: a Wide Range of Evolutions to Come
Motorisation et carburants Diesel : un large spectre d'évolutions à venir

Global Airpath Control for a Turbocharged Diesel HCCI Engine

J. Chauvin*, P. Moulin, B. Youssef and O. Grondin

Institut français du pétrole, IFP, 1-4 avenue de Bois-Préau, 92852 Rueil-Malmaison Cedex - France
e-mail: jonathan.chauvin@ifp.fr - philippe.moulin@ifp.fr - bilal.youssef@ifp.fr - olivier.grondin@ifp.fr
* Corresponding author

Résumé — Contrôle expérimental des boucles d'air et d'EGR d'un moteur HCCI suralimenté — Une stratégie de contrôle basée sur une planification de trajectoire est proposée pour la commande de la boucle d'air d'un moteur Diesel turbocompressé avec recirculation de gaz d'échappement (EGR). Le modèle considéré utilise des équations physiques simples de conservation de masse et d'énergie. La dynamique entièrement actionnée est facilement inversée, permettant de générer une loi de commande boucle ouverte. Un feedback est réalisé en utilisant un observateur pour les variables non directement mesurées. De plus, une stratégie de contrôle de la turbine est présentée afin de répondre rapidement aux demandes de débits d'air en tenant compte de la dynamique du turbocompresseur. Des essais au banc moteur ont été réalisés sur un moteur de 4 cylindres dans le mode de combustion homogène (HCCI). Les conclusions soulignent la possibilité de tenir compte des dynamiques de non-minimum de phase de ce système par un simple, pourtant efficace dedans pratique, loi de commande. Les transitoires réalisés sont précis et rapides.

Abstract* — *Global Airpath Control for a Turbocharged Diesel HCCI Engine *— A motion planning based control strategy is proposed for the airpath control of turbocharged Diesel engines using Exhaust Gas Recirculation (EGR). The considered model uses simple balance equations. The fully actuated dynamics are easily inverted, yielding straightforward open-loop control laws. This approach is complemented by experimentally derived look-up tables to cast the drivers requests into transients between operating points. Moreover, a turbocharging control strategy is developed to provide the required amount of fresh air taking into account the turbocharger dynamics. Experimental tests are reported on a 4-cylinder engine in Homogeneous Charge Compression Ignition (HCCI) mode. Conclusions stress the possibility of taking into account the non minimum phase effects of this system by a simple, yet efficient, control law. Realized transients are fast and accurate.*

INTRODUCTION

Several directions are investigated for the reduction of Diesel engines pollutant emissions, while maintaining a low fuel consumption. One of the solutions envisaged is the reduction of the pollutant produced in the cylinder during the combustion rather than adding more complex after treatment system. This is the objective of the HCCI Diesel engines which enable a drastic reduction of the nitric oxydes (NOx) thanks to high amounts of Exhaust Gas Recirculation (EGR). However, the potential benefits of HCCI combustion in terms of emissions are counterbalanced by its high sensitivity to in-cylinder thermodynamic conditions since the combustion is controlled by the chemical kinetics. The challenge with HCCI engines is to maintain the adequate conditions in the cylinders. The capacity to provide fresh air to the system even with high EGR rates makes necessary the use of advanced turbo charging systems. This has led to the development of complex air intake system architectures. In practice, numerous experimentations brought the proof of significant emission reduction (see [1, 2] for example). However, actual vehicle implementation implies frequent transients which are much more complex than steady state experimentation.

As studied in [3, 4], the airpath system of a turbocharged Diesel engine features coupled dynamics. The EGR acts as a discharge valve for the turbocharger. Most studies consider the following control setup: both intake pressure and intake air flow are closely controlled using EGR valve and Variable Geometry Turbocharger (VGT) using gain scheduling PI controllers as in [5-7]. The PI gains are tuned with respect of engine speed and fueling rate. PI gains are generated by the inverted plant gain at each operating point. Linear Parameter-Varying (LPV) formulation is used in [8, 9]. A LPV Diesel airpath model is derived from a simple nonlinear system and use H_∞ loopshaping control to regulate the intake pressure and the intake air flow. Controlling both intake and exhaust pressure has been exposed in [10]. In [11, 12], constructive Lyapunov technique is used to control the air-fuel ratio and EGR fraction to their respective set points determined by the operating conditions during quasi-steady state operation. For that purpose, intake pressure, intake mass air flow, and exhaust pressure measurements are used along with several change of coordinates.

All these studies prove the relevance of multivariable control strategies. In this paper, we use a motion planning strategy and explicit a feedforward term. Originally, our objective is to satisfy the drivers's torque demand. Successively, we cast it into in-cylinder masses setpoints, and into BGR (Burned Gas Rate) and intake manifold pressure control setpoints. An explicit unconstrained transient is computed. Thanks to tuning parameters, it is consistent with physically important constraints on the inputs. If not, it is saturated, and, as is proven, eventually provides convergence anyway.

The contribution of this paper is as follows. We present the overall control scheme for the airpath control of a turbocharged Diesel engine. This is the association of the air/EGR control presented in [13, 14] and the turbocharger control presented in [15]. Extensive experimental results are reported. At the light of this study, we can finally conclude, with supportive results, that motion planning is indeed an appropriate solution for controlling the airpath dynamics.

The paper is organized as follows. In Section 1, we detail the control problem. In Section 3, we decouple the airpath fully actuated dynamics by a simple motion planning strategy. The motion planning strategy leads to control the EGR flow with the EGR valve and the air flow with the turbocharger. The turbocharging control is detailed in Section 4. Experimental results are reported on a 4 cylinder HCCI engine in Section 5. Conclusions and future directions are given in Section 6.

1 CONTROL PROBLEM

Our approach to combustion control is to manage the air and burned gas masses in the cylinder ($M_{air,cyl}$ and $M_{bg,cyl}$). In other words, we focus on the airpath system. Flows of fresh air and the Exhaust Gas Recirculation (EGR) mix into the intake manifold and are aspirated into the cylinders. In practical applications, the considered masses cannot be measured. However, equivalent variables can be considered. Controlling those two masses is equivalent to controlling the intake pressure P_{int} (being an image of $M_{air,cyl} + M_{bg,cyl}$) and the burned gas rate F_{int} (representing to ratio $\frac{M_{bg,cyl}}{M_{air,cyl}+M_{bg,cyl}}$). Setpoints are often chosen to maximize EGR in order to lower the NO_x emissions from low load to part load. At high load, the EGR decreases the efficiency and thus we use lower EGR levels. Typically, the setpoint at 1500 rpm and high load is ($P_{int,sp} = 2$ bar, $F_{int,sp} = 0.05$) using low EGR, while at 1500 rpm and low load setpoints under consideration are close to ($P_{int,sp} = 1.013$ bar, $F_{int,sp} = 0.45$) using high EGR.

The function of the turbocharger system is to transfer part of the exhaust gas energy to the intake gases and thus increase the overall engine efficiency. The turbine uses this stored energy to produce mechanical torque which drives the compressor via the shaft. The intake pressure is thus increased, which allows to run the engine on a wider operating range than a naturally aspirated engine.

In this context, the control issue is to manage large transients for a MIMO system with 2 inputs and 2 outputs. The control inputs are the VGT actuator position $S_{vgt}(v_1)$ (ranging from 0 to 1) and the EGR valve normalized effective area $S_{egr}(v_2)$ (ranging from 0 to 1). Both are bounded. Other external inputs include the fueling rate M_{fuel} and the engine speed N_e. The underlying dynamics is also of dimension 2. The states are the outputs: P_{int} and F_{int}.

2 INTAKE MANIFOLD MODELLING

Flows from the fresh air (measured by the Manifold Air Flow) and the Exhaust Gas Recirculation come into the intake manifold and are aspirated into the cylinders. To describe this system, we use a mean value engine model based on mass balances, ideal gas law, and consider a low time resolution (180° TDC time scale). In particular, high frequency aspiration phenomena are not taken into account.

Ideal gas law in the intake manifold leads to

$$P_{int}V_{int} = M_{int}RT_{int}$$

Assuming that the variation of temperature is slow (*i.e.* $\dot{T}_{int} = 0$), the mass balance writes

$$\dot{P}_{int} = \frac{RT_{int}}{V_{int}}(D_{air} + D_{egr} - D_{asp}) \tag{1}$$

Classically (see [16] for exemple), we define the aspirated flow as

$$D_{asp} = \eta_{vol}(P_{int}, N_e)\frac{P_{int}}{RT_{int}}V_{cyl}\frac{N_e}{120} \tag{2}$$

where V_{cyl} is the cylinder volume. η_{vol} is the volumetric efficiency which is experimentally derived and, eventually, defined though a 2-D look-up table $\eta_{vol,map}(P_{int}, N_e)$. Values vary with engine operating conditions (mainly intake pressure and engine speed).

The burned gas ratio F_{int} is the fraction of burned gas in the intake manifold. It is written as

$$F_{int} \triangleq 1 - \frac{M_{int,air}}{M_{int}}$$

The composition of the EGR (F_{egr}) is the composition in the exhaust manifold (F_{exh}) delayed by the transport through the EGR pipe. We consider that this delay is negligible, *i.e.* $F_{egr} = F_{exh}$. Mixing dynamics is modelled as

$$\dot{F}_{int} = \frac{RT_{int}}{P_{int}V_{int}}(D_{egr}(F_{exh} - F_{int}) - D_{air}F_{int}) \tag{3}$$

The EGR flow can be expressed as

$$D_{egr} = S_{egr}\frac{P_{exh}}{\sqrt{RT_{exh}}}\sqrt{\frac{2\gamma}{\gamma - 1}\left(p_r^{\frac{2}{\gamma}} - p_r^{\frac{\gamma-1}{\gamma}}\right)}$$

where $p_r = \max\{\frac{P_{int}}{P_{exh}}, (\frac{2}{\gamma+1})^{\frac{\gamma}{\gamma+1}}\}$. These two variables describe both subsonic and choked EGR flow. In this model, numerous variables are not measured. The exhaust pressure and temperature for example are not easily available on a commercial engine. The effect of the EGR cooler is accounted for by considering

$$D_{egr} \triangleq \Theta_{egr}S_{egr}$$

where Θ_{egr} is a variable depending on the exhaust temperature, the pressure ratio between intake and exhaust manifold, and the behavior of the cooling system. This variable needs to be estimated to evaluate the EGR flow and the composition in the intake manifold. An observer for these quantities is proposed in [13].

3 AIR PATH CONTROL STRUCTURE

The airpath structure follows the strategy presented in [13, 14].

3.1 Feedforward Strategy

The control inputs we consider are the EGR flow D_{egr} and the fresh air flow D_{air}. The reference model for the control is written as

$$\begin{cases} \dot{x}_1 = \alpha_{int}\,(u_1 + u_2 - \eta_{vol}(x_1, N_e)\beta_{int}x_1) \\ \dot{x}_2 = \frac{\alpha_{int}}{x_1}\,(F_{exh}u_2 - (u_1 + u_2)x_2) \end{cases} \tag{4}$$

We propose a motion planning control strategy which relies on the computation of transient trajectories for the airpath dynamics 4. This strategy is detailed in Figure 4. It comprises 4 sub procedures:

- setpoint computations through static maps (first two blocks in Fig. 4);
- trajectory generation;
- model inversion;
- saturation of open-loop control values.

We now detail these in the next subsection.

3.1.1 Set Points

The driver's request considered here is the accelerator position. First, taking into account the gear box configuration, this request is turned into a torque control objective under the form of an IMEP (Indicated Mean Effective Pressure) set point. Then, the set points for the intake pressure and the BGR (noted x^{sp} in Fig. 4) are inversely given by experimentally calibrated static maps on the $(\text{IMEP}^{\text{sp}}, N_e)$ operating range. The engine speed N_e is not modelled but directly measured. The $x^{\text{sp}} = (x_1^{\text{sp}}, x_2^{\text{sp}})$ vector is defined as

$$x_1^{\text{sp}} = f_{\text{pressure}}(\text{IMEP}^{\text{sp}}, N_e) \text{ and } x_2^{\text{sp}} = f_{\text{bgr}}(\text{IMEP}^{\text{sp}}, N_e)$$

3.1.2 Motion Planning

Because IMEP^{sp} is arbitrarily specified by the driver, $t \mapsto x_1^{\text{sp}}(t)$ and $t \mapsto x_2^{\text{sp}}(t)$ may not be smooth nor monotonous. These signals must be filtered to correspond to feasible trajectories of 4. This can be done by many methods. Here, we propose the following approach that, besides other interesting properties, is easy to handle in the convergence analysis process. It addresses only the case of transients from one steady state to another. From a current steady state $\underline{x}$ to a target $\overline{x}$ we use an interpolation formula 5. Coordinate-wise this defines x_1^{mp} and x_2^{mp}. Let

$$\phi(t, T) = \begin{cases} 0 & \text{for } 0 \geq t \\ (\frac{t}{T})^2(3 - 2\frac{t}{T}) & \text{for } 0 \leq t \leq T \\ 1 & \text{for } T \leq t \end{cases} \tag{5}$$

Note two positive constants T_1 and T_2. The considered interpolation is

$$\begin{cases} x_1^{\text{mp}}(t) = \underline{x}_1 + (\overline{x}_1 - \underline{x}_1)\phi(t, T_1) \\ x_2^{\text{mp}}(t) = \underline{x}_2 + (\overline{x}_2 - \underline{x}_2)\phi(t, T_2) \end{cases} \quad (6)$$

3.1.3 Model Inversion

System 4 is fully actuated and invertible. Thus, an analytic expression of the input can be derived from the state variables and their first derivatives histories. In fact,

$$\begin{cases} u_1 + u_2 = \eta_{vol}(x_1, N_e)\beta_{int}x_1 + \frac{1}{\alpha_{int}}\dot{x}_1 \\ -x_2u_1 + (F_{exh} - x_2)u_2 = \frac{1}{\alpha_{int}}\dot{x}_2x_1 \end{cases} \quad (7)$$

This rewrites as

$$\begin{cases} u_1 = f_1(x, \dot{x}) \\ u_2 = f_2(x, \dot{x}) \end{cases} \quad (8)$$

with

$$\begin{cases} f_1(x, \dot{x}) = \frac{1}{F_{exh}}(\frac{F_{exh}-x_2}{\alpha_{int}}\dot{x}_1 - \frac{1}{\alpha_{int}}\dot{x}_2x_1 \\ \qquad\qquad +(F_{exh} - x_2)\eta_{\text{vol}}(x_1, N_e)\beta_{int}x_1) \\ f_2(x, \dot{x}) = \frac{1}{F_{exh}}(\frac{1}{\alpha_{int}}x_2\dot{x}_1 \\ \qquad\qquad +\eta_{\text{vol}}(x_1, N_e)\beta_{int}x_2x_1 + \frac{1}{\alpha_{int}}\dot{x}_2x_1) \end{cases} \quad (9)$$

In these last expressions, F_{exh}, α_{int}, N_e, and β_{int} are all given by sensors measurements. The unique open-loop control law $(u_1^{\text{mp}}, u_2^{\text{mp}})$ corresponding to any desired $(x_1^{\text{mp}}, x_2^{\text{mp}})$ trajectory (defined by formulas 6) is

$$\begin{cases} u_1^{\text{mp}} = f_1(x_1^{\text{mp}}, \dot{x}_1^{\text{mp}}, x_2^{\text{mp}}, \dot{x}_2^{\text{mp}}) \\ u_2^{\text{mp}} = f_2(x_1^{\text{mp}}, \dot{x}_1^{\text{mp}}, x_2^{\text{mp}}, \dot{x}_2^{\text{mp}}) \end{cases} \quad (10)$$

The calibration of the tuning parameters T_1 and T_2 is proposed in [18].

3.2 Feedback Strategy

Fast PID controllers are added to the structure to provide further accuracy and robustness. The goal of the feedback is to control the EGR flow D_{egr} and the air flow D_{air} toward the reference setpoints D_{egr}^{ol} and D_{air}^{ol}. The main purpose of the feedforward is to give a feasible and continuous setpoint for the feedback action.

3.2.1 EGR Position to D_{egr}

Increasing the EGR position corresponds to opening the EGR valve and, thereby, increasing the EGR flow D_{egr}. The flow response is almost instantaneous, the EGR valve opening control the EGR flow D_{egr}. More precisely, a PI controller with an anti-wind up action on the normalized EGR flow $(\frac{D_{\text{egr,sp}} - \hat{D}_{\text{egr}}}{\hat{\Theta}_{egr}})$ is used on the EGR valve.

TABLE 1

Variation of air/EGR flows depending on VGT

Low EGR		
Decreasing VGT	⇒	High increasing D_{air}
	⇒	Low increasing D_{egr}
High EGR		
Decreasing VGT	⇒	Low decreasing D_{air}
	⇒	Low increasing D_{egr}

3.2.2 VGT to D_{air}

Increasing the VGT position, *i.e.* opening the guide vanes, leads to a greater restriction of the exhaust gas flow and then to a decrease of the exhaust manifold pressure.

When the EGR valve is wide open (at low speed and low load *e.g.*), increasing the VGT results in a decreased EGR flow D_{egr} which in turn increases the air flow D_{air}. The EGR and air flow variations according to the VGT positions are summarized in Table 1.

When the EGR valve is almost closed, most of the exhaust gas must pass through the turbine. Increasing the VGT decreases the compressor power and, then, increases the air flow. In this case, the VGT acts as a conventional wastegate, *i.e.* the VGT directly controls the turbocharger speed and the air flow D_{air}. Therefore, the steady-state gain from VGT to D_{air} undergoes a sign change depending on the operating point. Since it is uncertain where the sign change occurs, the VGT should not be used to track D_{air} setpoints in a decentralized strategy. Rather, the strategy should use the EGR flow information. The variation of intake pressure is monotonic w.r.t. VGT. Depending on the opening of the EGR valve, *i.e.* depending on the EGR flow, the variation of pressure is very different. Indeed, in practice, with very high EGR rate, the variation of the VGT slightly impact the intake pressure. A tedious calibration work is a solution. Instead, we propose a global control of the turbocharger as described in the next section.

4 TURBOCHARGER CONTROL STRUCTURE

The modelling and the control strategy follow [15].

4.1 System Modelling

The evolution of the turbocharger rotational speed N_t is derived from the power balance on the turbocharger shaft. For the sake of simplicity the friction losses are neglected:

$$P_t - P_c = J_tN_t\frac{dN_t}{dt} \quad (11)$$

where J_t is the moment of inertia of the rotating parts. The power developed by the turbine P_t and the power required

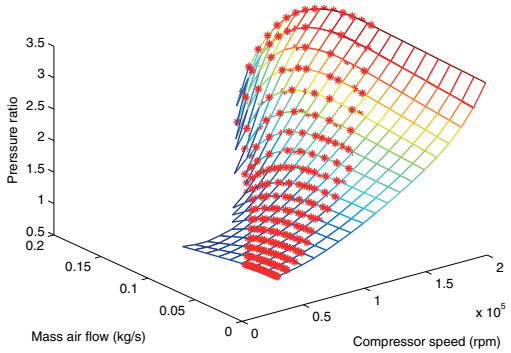

Figure 1

Compressor pressure ratio map.

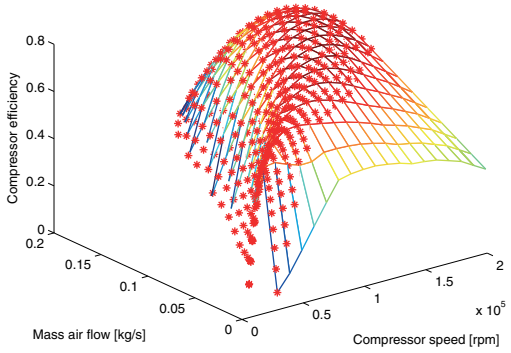

Figure 2

Compressor efficiency map.

to drive the compressor P_c can be expressed as follow:

$$P_t = D_t c_p \eta_t T_{ut} \left[1 - \left(\frac{1}{PR_t} \right)^{\frac{\gamma-1}{\gamma}} \right] \tag{12}$$

$$P_c = D_{air} c_p \frac{1}{\eta_c} T_{uc} \left[PR_c^{\frac{\gamma-1}{\gamma}} - 1 \right] \tag{13}$$

where D_t, is the turbine flow (we recall that D_{air} is the compressor flow), η_t, η_c are the turbine and compressor efficiencies and PR_t, PR_c are the turbine and compressor pressure ratios, respectively. c_p is the specific heat at constant pressure. The compressor efficiency and pressure ratio are given by steady static maps which depend on corrected compressor speed and mass flow. These maps characterize a given compressor, they are provided by the manufacturer (see Figs. 1, 2).

$$PR_c = f_1 \left(D_{air} \frac{\sqrt{T_{uc}} P_{ref}}{\sqrt{T_{ref}} P_{uc}}, N_t \frac{\sqrt{T_{ref}}}{\sqrt{T_{uc}}} \right)$$

$$\eta_c = f_2 \left(D_{air} \frac{\sqrt{T_{uc}} P_{ref}}{\sqrt{T_{ref}} P_{uc}}, N_t \frac{\sqrt{T_{ref}}}{\sqrt{T_{uc}}} \right)$$

T_{ref} is a constant reference temperature. Similar maps are used for the turbine, except that the actuation of the VGT has an impact on the turbine characteristics. The corrected turbine flow can be represented as a function of the corrected turbine speed, pressure ratio and VGT actuator position. P_{ref} is a constant reference pressure.

$$D_t \frac{\sqrt{T_{ut}} P_{ref}}{\sqrt{T_{ref}} P_{ut}} = f_3 \left(PR_t, N_t \frac{\sqrt{T_{ref}}}{\sqrt{T_{ut}}}, u_{vgt} \right)$$

$$\eta_t = f_4 \left(D_t \frac{\sqrt{T_{ut}} P_{ref}}{\sqrt{T_{ref}} P_{ut}}, N_t \frac{\sqrt{T_{ref}}}{\sqrt{T_{ut}}}, u_{vgt} \right)$$

The set of equations from 11 to 4.1 provides a simple representation of the system behavior. They are widely used in publications dealing with turbocharger modelling (for example [19] and [20]).

We will make the strong hypothesis that the dynamics of the intake and exhaust manifold can be neglected because they are much faster than the ones of the turbocharger system. This simplifies the equations above, which become:

$$D_t = D_{asp} + D_f \tag{14}$$

Where D_f is a small flow due to the fuel injection. Equations 11–14 describe a system with one state and many time dependant non linearities. This representation has to be further simplified to be used directly in control algorithms.

4.2 Turbocharger Control Strategy

Since the system state is the turbocharger speed, the choice of this variable as a control variable proves to be interesting. Furthermore, it can be noticed that the map of Equation 4.1 is invertible and that the turbocharger speed can be written as a function which depends on compressor pressure ratio and mass air flow:

$$N_t = f_5 \left(D_{air} \frac{\sqrt{T_{uc}} P_{ref}}{\sqrt{T_{ref}} P_{uc}}, PR_c \right) \frac{\sqrt{T_{uc}}}{\sqrt{T_{ref}}} \tag{15}$$

The intake pressure setpoint is transformed into a compressor pressure ratio setpoint which gives the turbocharger speed setpoint using inverted compressor map. Consequently, our goal is to control the turbocharger system such that the turbocharger speed N_t follows its reference signal $N_{t,d}$ as closely as possible. This is the aim of this section. The control law may be designed by exploiting the structure of Equations 11–13 to derive a back-stepping based control law. By taking

$$\begin{cases} \alpha_t = \frac{2}{J_t} D_t c_p \eta_t T_{ut} \\ \beta_c = \frac{2}{J_t} P_c \\ u_t = 1 - \left(\frac{1}{PR_t} \right)^{\frac{\gamma-1}{\gamma}} \\ y = N_t^2 \end{cases} \tag{16}$$

Equation 11 can be written in the following form:

$$\alpha_t u_t - \beta_c = \frac{dy}{dt} \tag{17}$$

Note that the parameters α_t and β_t in Equation 17 can be calculated using measured variables and turbocharger efficiency maps. Since the turbine and compressor efficiencies vary slowly with the turbocharger speed, they will be considered to be constant in the control law. This system is time varying and non linear. But it is trivial that it is flat [21]: a simple equation links the flat output y (square of the turbocharger speed) with the input u (function of the exhaust pressure). By a simple technique of back stepping it is possible to force the system to follow its setpoint with an exponential decay given by Equation 18: the control law has to be defined as in Equation 19 (obtained directly by applying *Equations 17 and 18*).

$$\frac{d(y - y_d)}{dt} = -\mu(y - y_d) \tag{18}$$

$$u_t = \frac{1}{\alpha_t}\left(\frac{dy_d}{dt} - \mu(y - y_d) + \beta_c\right) \tag{19}$$

The derivative term corresponds to a dynamic feed forward term. The reference trajectory y_d should be filtered in order to respect physical constraints of the system. Here, a second order low pass filter has been used, where the damping and pulsation coefficients are set to fit the characteristic settling time. An extension of this work is to introduce the actuator constraints into the motion planning. In Equation 18, μ is a proportional gain and the reference signal is given by

$$y_d = N_{t,d}^2 \tag{20}$$

An integral term can be added to Equation 19 in order to compensate for modelling error. The final control law is then obtained:

$$u_t = \frac{1}{\alpha_t}\left(\frac{dy_d}{dt} - \mu(y - y_d) + \beta_c + \lambda\int(y - y_d)\right) \tag{21}$$

In a second stage, the real actuator command has to be computed from this control law that ensures a good setpoint tracking. The desired turbine pressure ratio can be deduced from Equations 16 and 21 as follow:

$$PR_t^d = (1 - u_t)^{\frac{\gamma}{1-\gamma}} \tag{22}$$

Finally, the VGT position is computed from the desired turbine pressure ratio. This is done by approximating the turbine maps with the following equations:

$$D_t = \Big(aG(u_{vgt}) + b\Big)\psi(PR_t) \tag{23}$$

Where $G(u_{vgt})$ is a bijective polynomial function of u_{vgt} and:

$$\psi(PR_t) = \sqrt{\frac{2\gamma PR_t}{r(\gamma - 1)}}\sqrt{PR_t^{\frac{-2}{\gamma}} - PR_t^{\frac{-\gamma-1}{\gamma}}} \tag{24}$$

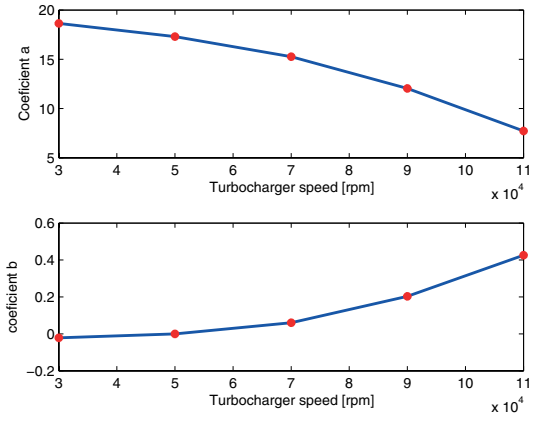

Figure 3

Values of the coefficients a and b according to the turbocharger speed.

γ is the specific heats ratio. The two parameters a and b are identified off-line from the characteristic turbine maps using optimization methods. They depend on the turbocharger speed only, but this dependence is slow and can be taken into account in the strategy. The parameter b can be corrected on line by an integrator to compensate modelling errors. The interpretation of Equations 23 and 24 is that the turbine is represented as an orifice with a section depending on the VGT position. The standard equations giving the mass flow rate as a function of pressure ratio have been slightly modified in order to fit the turbine maps. Figure 3 shows the coefficients a and b obtained as a function of the corrected turbine speed. We now have separated the effects of the VGT command, turbocharger speed and pressure ratio in equation

$$D_t\frac{\sqrt{T_{ut}}P_{ref}}{\sqrt{T_{ref}}P_{ut}} = f_3\left(PR_t, N_t\frac{\sqrt{T_{ref}}}{\sqrt{T_{ut}}}, u_{vgt}\right)$$

and obtained Equation 23 which is invertible. It is possible to express the VGT command that respects the control law defined in Equation 21. It is noticeable that the influence of the EGR system is implicitly taken into account. The fast dynamics are neglected as explained above, but the steady state effects on the VGT command are taken into account. We have obtained a control law with the desired features: a feed forward term based on a physical model accounting for the influences of other phenomena, and a limited number of tuning parameters.

5 EXPERIMENTAL RESULTS

5.1 Implementation

The global control scheme is summarized in Figure 4.

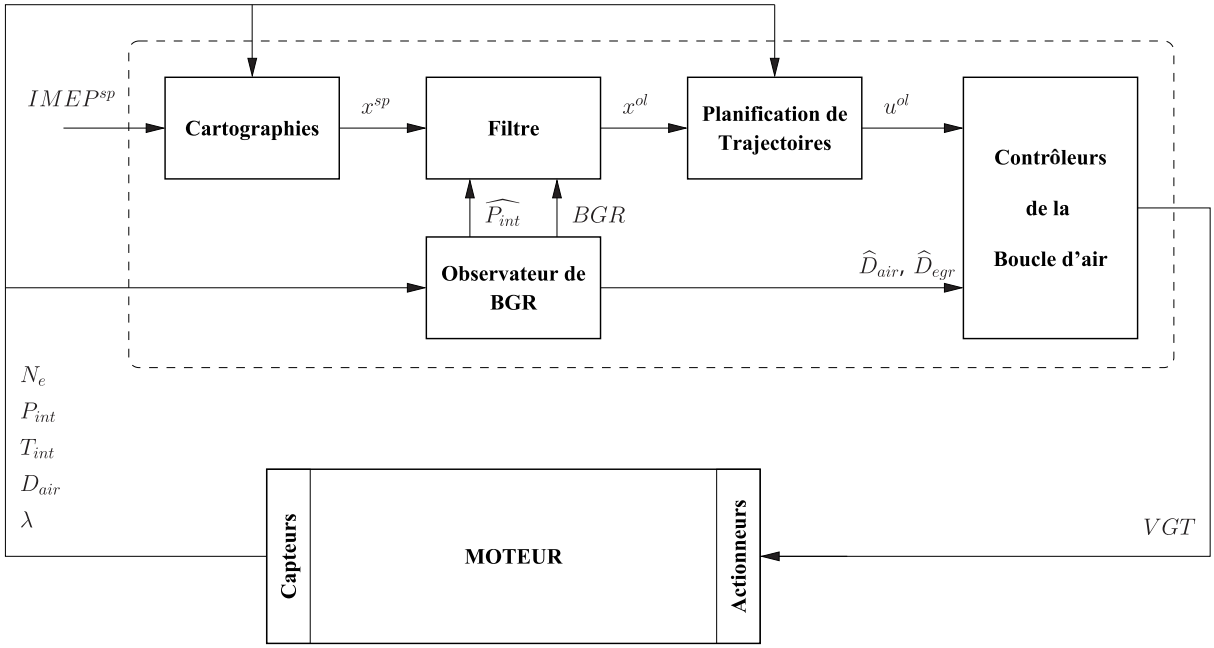

Figure 4

Control scheme.

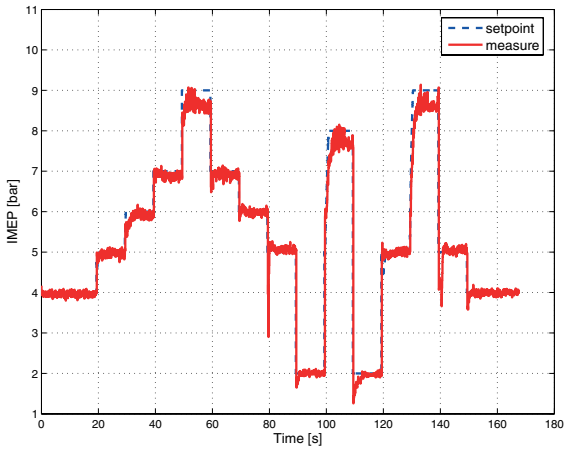

Figure 5

Experimental torque trajectory at constant engine speed (2500 rpm). Dashed: set point, solid: closed-loop trajectory.

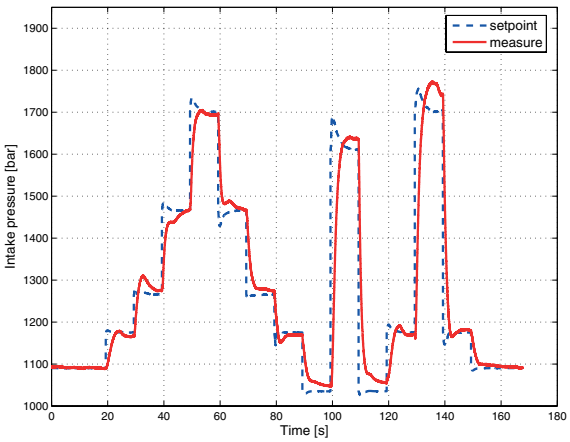

Figure 6

Experimental results on a torque trajectory at constant engine speed (2500 rpm): Intake pressure histories. Dashed: set point, solid: closed-loop trajectory.

The control was tested on torque trajectory at fixed engine speed (2500 rpm). This torque trajectory mixes HCCI combustion mode (for $\text{IMEP}_{sp} < 7$ bar) and conventional combustion mode. The same calibration was kept on all the torque trajectory. The IMEP demand is displayed in Figure 5. The intake pressure and BGR set points and closed-loop trajectories are presented in Figures 6 and 7. Actuators trajectories are reported in Figure 8.

The air and EGR flows setpoints and closed-loop trajectory are presented in Figures 9 and 10. As in the following cases, the EGR flow is almost perfectly tracked, the air flow tracking is good but slower during large transients due to

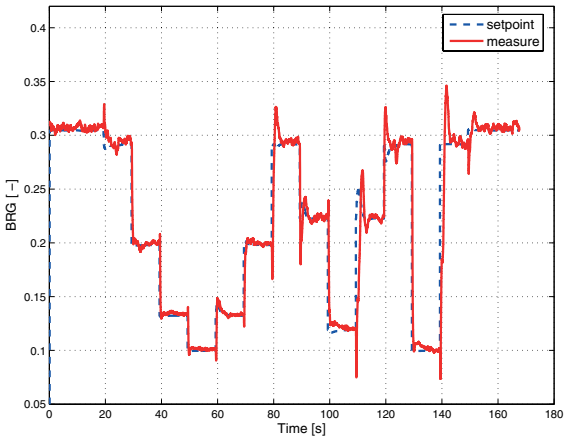

Figure 7

Experimental results on a torque trajectory at constant engine speed (2500 rpm): BGR histories. Dashed: set point, solid: closed-loop trajectory.

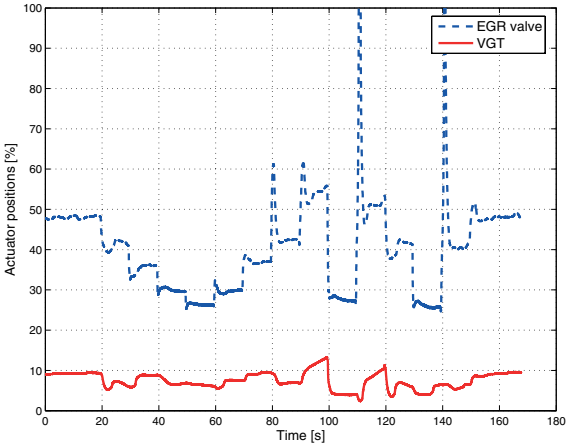

Figure 8

Experimental results on a torque trajectory at constant engine speed (2500 rpm): Actuators histories. Dashed: EGR valve, solid: VGT.

the turbocharger inertia. In summary, the results are good, even with a reasonably large transient. We are able to follow the planned trajectory. High pressure setpoints are more difficult to reach due to the turbocharger inertia and friction. However, it is possible to relax the intake pressure tracking because, for pollutant reduction purposes, only BGR needs to be closely controlled provided a limited Air-Fuel Ratio is guaranteed. The errors on the intake pressure will only lead to a very small error on the torque production. Nevertheless, on a vehicle, this problem will not appear because as the torque production increases, in response, the engine speed and the turbocharger speed increases. This phenomenon is expected to be reduced in real-vehicle applications.

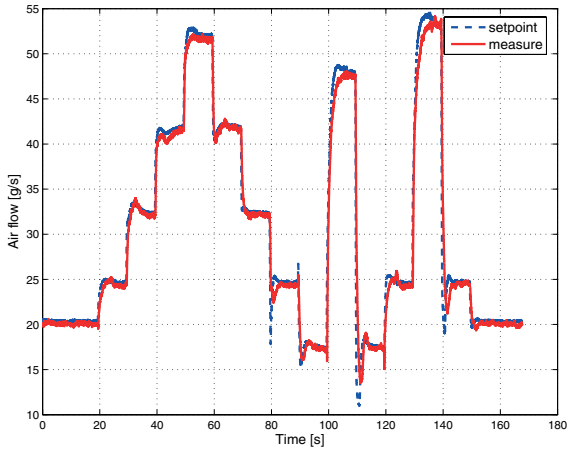

Figure 9

Experimental results on a torque trajectory at constant engine speed (2500 rpm): Air flow histories. histories. Dashed: set point, solid: closed-loop trajectory.

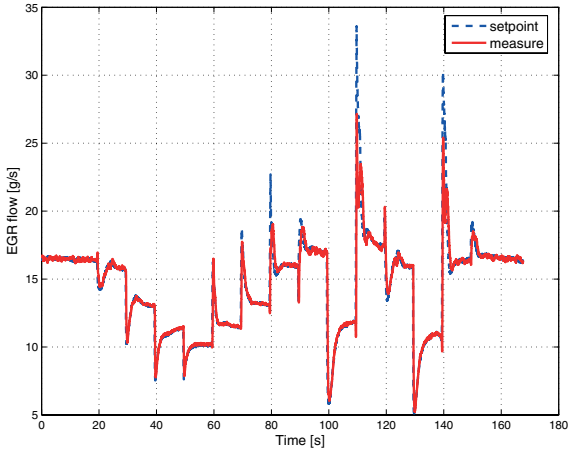

Figure 10

Experimental results on a torque trajectory at constant engine speed (2500 rpm): EGR flow histories. histories. Dashed: set point, solid: closed-loop trajectory.

6 CONCLUSIONS AND FUTURE WORK

6.1 Conclusion

The presented work demonstrates the relevance of motion planning in the control of the – coupled – airpath dynamics of turbocharged Diesel engines using Exhaust Gas Recirculation. For the HCCI combustion mode, very large rates of burned gas need to be considered and we have proven on realistic test-bench cases that the proposed approach can handle such situations. The proposed control strategy has several advantages.

– Its multivariable construction takes the non minimum phase behavior of the system.
– The dynamic feedforward strategy allows the possibility of very fast transients.
– The model based turbocharger control decrease the turbocharger response time by taking the inertia into account.

6.2 Toward General Airpath Control

The presented work is validated experimentally on a HCCI engine with a high pressure EGR circuit and a Variable Geometry Turbocharger. The next step is the extension of the control strategy to other engine configurations, e.g. considering low pressure EGR circuit, waste-gate, two-stage turbocharger, intake throttle... The control strategy can be kept. The observer will be the same (in Fig. 4), and so will the motion planning. The main modification will be to decentralize the control in order to use all the actuators for the control of the air flow D_{air} and the EGR flow D_{egr}.

REFERENCES

1 Kahrstedt J., Behnk K., Sommer A., Wormbs T. (2003) Combustion processes to meet future emission standards, Motortech. Zeitschrift, pp. 1417–1423.

2 Hultqvist A., Engdar U., Johansson B., Klingmann J. (2001) Reacting boundary layers in a homogeneous charge compression ignition HCCI) engine, *Proc. of the SAE Conference*, number 2001-01-1032.

3 Kolmanovsky I., Stefanopoulou A., Moraal P., van Nieuwstadt M. (1997) Issues in modelling and control of intake flow in variable geometry turbocharged engines, In *Proc. of the 18th IFIP Conference on System Modelling and Optimization*.

4 Kao M., Moskwa J. (1995) Turbocharged Diesel engine modelling for nonlinear engine control and estimation, *ASME J. Dynamic Syst., Meas. and Control*, 117.

5 van Nieuwstadt M., Moraal P., Kolmanovsky I., Stefanopoulou A., Wood P., Criddle M. (1998) Decentralized and multivariable designs for EGR-VGT control of Diesel engine, *Proc. of the 2nd IFAC Workshop on Advances in Automotive Control*.

6 Stefanopoulou A., Kolmanovsky I., Freudenberg J. (2000) Control of variable geometry turbocharged Diesel engines for reducted emissions, *IEEE T. Contr. Syst. T.* **8**, 733–745.

7 van Nieuwstadt M., Kolmanovsky I., Moraal P., Stefanopoulou A., Janković M. (2000) Experimental comparison of EGR-VGT control schemes for a high speed Diesel engine, *Control Syst. Mag.* **20**, 63–79.

8 Jung M., Glover K. (2003) Control-oriented linear parameter-varying modelling of a turbocharged Diesel engine, *Conference on Control Application*.

9 Jung M., Glover K. (2005) Comparison of uncertainty parameterisations for H-infinity robust control of turbocharged Diesel engines, *Control Eng. Pract.* **13**, 15–25.

10 Ammann M., Fekete N., Guzzella L., Glattfelder A. (2003) Model-based control of the VGT and EGR in a turbocharged common-rail Diesel engine: theory and passenger car implementation, *Proc. of the SAE Conference*, number 2003-01-0357.

11 Janković M., Kolmanovsky I. (1998) Robust nonlinear controller for turbocharged Diesel engine, *Proc. of the American Control Conference*.

12 Janković M., Kolmanovsky I. (2000) Constructive Lyapounov control design for turbocharged Diesel engines, *IEEE T. Contr. Syst. T.* **8**, 288–299.

13 Chauvin J., Corde G., Petit N., Rouchon P. (2007) Airpath strategy for experimental transient control of a Diesel HCCI engine, *Oil Gas Sci. Technol.* **62**, 4, 483–491.

14 Chauvin J., Corde G., Petit N., Rouchon P. (2008) Motion planning for experimental air path control of a Diesel HCCI engine, *Control Eng. Pract.* (in press).

15 Youssef B., Moulin P., Grondin O. (2007) Model based control of turbochargers: Application to a diesel HCCI engine, *Conference on Control Application*.

16 Heywood J. (1998) *Internal Combustion Engine Fundamentals*, McGraw-Hill, Inc.

17 Chauvin J., Corde G., Vigild C., Petit N., Rouchon P. (2006) Air path estimation on Diesel HCCI engine, *Proc. of the SAE Conference*, number 2006-01-1085.

18 Chauvin J., Corde G., Petit N. (2006) Constrained motion planning for the airpath of a Diesel HCCI engine, *Proc. of the IEEE Conf. Decision and Control*.

19 Jensen J-P. , Kristensen A.F. , Sorenson S.C. , Houbak N. Hendricks E. (1991) Mean value modelling of a small turbocharged diesel engine, *Proc. of the SAE Conference*, number 910070.

20 Moraal P., Kolmanovsky I. (1999) Turbocharger modeling for automotive control applications, *Proc. of the SAE Conference*, number 1999-01-0908.

21 Fliess M., Lévine J., Martin P., Rouchon P. (1995) Flatness and defect of nonlinear systems: Introductory theory and examples, *Inte. J. Control* **61**, 1327–1361.

Final manuscript received in June 2008
Published online in August 2008